IOP PUBLISHING METROLOGIA
Metrologia **46** (2009) S139–S145 doi:10.1088/0026-1394/46/4/S01

Radiometer standard for absolute responsivity calibrations from 950 nm to 1650 nm with 0.05% ($k = 2$) uncertainty

G P Eppeldauer, H W Yoon, Y Zong, T C Larason, A Smith and M Racz

National Institute of Standards and Technology, Gaithersburg, MD, USA

Received 28 October 2008
Published 2 June 2009
Online at stacks.iop.org/Met/46/S139

Abstract
A near-IR radiometer standard with similar performance to silicon trap detectors has been developed to calibrate detectors and radiometers for absolute spectral power, irradiance and radiance responsivities between 950 nm and 1650 nm. The new radiometer standard is utilized at the Spectral Irradiance and Radiance Responsivity Calibrations using Uniform Sources (SIRCUS) which is the reference calibration facility of NIST for absolute responsivity. The radiometer standard is a sphere detector with a unique geometrical arrangement and it can convert the radiant power responsivity scale of the primary-standard cryogenic radiometer into a reference irradiance responsivity scale. The 0.05% ($k = 2$) scale conversion uncertainty is dominated by the two largest uncertainty components of the radiometer: the spatial non-uniformity of responsivity of less than 0.05% in power mode and the 0.03% angular responsivity deviation from the cosine function in a 5° angular range in irradiance mode. These small uncertainty components are the results of a tilted input aperture (relative to the sphere axis) and four symmetrically positioned InGaAs detectors around the incident beam spot in the sphere. With the new radiometer standard, it is expected that a thermodynamic temperature uncertainty of 10 mK ($k = 2$) can be achieved at 157 °C, the freeze temperature of the In fixed-point blackbody.

(Some figures in this article are in colour only in the electronic version)

1. Introduction

The primary basis of modern radiometry is the measurement of optical power with a cryogenic electrical-substitution radiometer. The spectroradiometric quantities such as spectral irradiance and spectral radiance can be derived from the primary power measurements. However, the derivation of the spectroradiometric quantities from optical power requires the use of spatially uniform and Lambertian detectors. These detectors serve as power-to-irradiance converters. In the visible and near-infrared (NIR) wavelength regions, up to 960 nm, silicon trap detectors, introduced in 1983 [1], are the lowest uncertainty transfer standards. Using these silicon reference detectors, 0.06% ($k = 2$) uncertainty can be achieved in irradiance measurement mode [2]. In the NIR region, between 950 nm and 1650 nm, where the use of Si detectors is not possible, trap detectors using either Ge or InGaAs photodiodes have been constructed [3, 4]. Since the Ge or InGaAs photodiodes have much smaller shunt resistances than Si, the combinations of large area, NIR diodes in parallel electrical connections have resulted in low shunt-resistance devices with much worse radiometric and electronic performances than Si trap detectors [5]. Also, the spatial non-uniformity of the internal-quantum-efficiency limited their power measurement uncertainties to about 0.3% ($k = 2$).

Another approach to obtain detectors with high spatial uniformity and Lambertian angular responsivity is to utilize an integrating sphere as the input to detectors which are directly attached to the sphere. Previous designs using InGaAs photodiodes have utilized either a single photodiode placed perpendicularly to the entrance aperture or multiple diodes facing the sphere centre [6, 7].

Among other applications, the need for low-uncertainty radiance responsivity calibrations is driven by the possible thermodynamic temperature realizations in the NIR wavelength region where a 0.05% ($k = 2$) absolute radiance responsivity

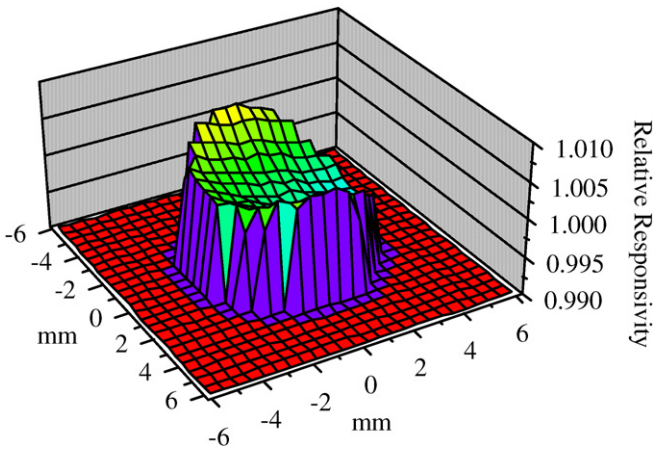

Figure 1. Spatial uniformity of responsivity of a traditional Ge sphere detector at 1500 nm.

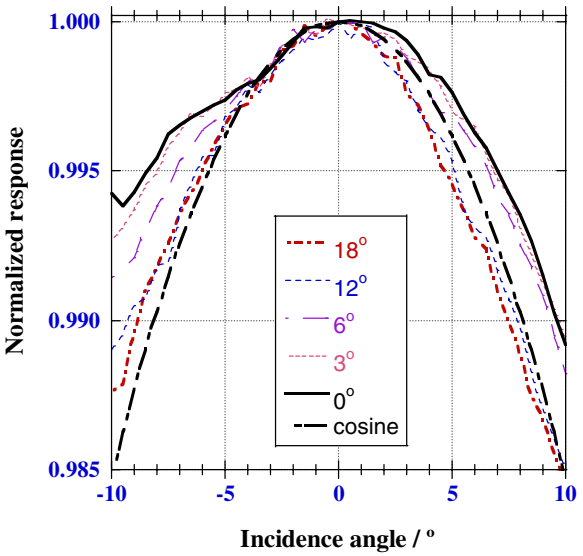

Figure 2. Angular response of a Ge sphere detector at different tilt angles of the input-aperture plane relative to the sphere axis.

uncertainty is needed to achieve a 10 mK ($k = 2$) uncertainty in the measurement of the In-point freezing blackbody at 157 °C. In the last 25 years, these low uncertainty requirements could not be achieved with regular NIR detectors; it was possible only with silicon trap detectors up to 960 nm. In order to achieve this low uncertainty in the NIR, a new type of power-to-irradiance converting radiometer standard is needed that will not limit the uncertainty of the spectral responsivity propagation from the primary-standard cryogenic radiometer. This new radiometer will be the reference detector of the Spectral Irradiance and Radiance Responsivity Calibrations using Uniform Sources (SIRCUS) facility for the NIR range where up until now these low-uncertainty spectral responsivity calibrations could not be performed.

We describe the design and characterization of a novel NIR radiometer transfer standard that makes it possible to perform spectral power and irradiance responsivity calibrations with uncertainties lower than 0.05% ($k = 2$).

2. Preliminary sphere-detector experiments

For spatial and angular responsivity tests, a Ge radiometer was attached to the exit port of a 5 cm diameter Spectralon[1] coated integrating sphere with 90° angle between the entrance and exit ports. The spatial uniformity of this simple (no baffles) and asymmetric Ge sphere detector with an 8 mm diameter input aperture is shown in figure 1. The aperture plane was (traditionally) normal to the sphere axis. The obtained maximum non-uniformity is 0.6% at 1500 nm using a 1.1 mm diameter scanning beam with 0.5 mm increments. The poor uniformity is caused by the asymmetric arrangement of the sphere input and output ports.

The angular responsivity test was performed with the same sphere-detector arrangement, but the sphere-aperture diameter was decreased to 3.5 mm to obtain improved sphere performance and better Lambertian angular response. First, as in traditional sphere-detector designs, the aperture plane was normal (0° tilt) to the sphere optical axis. The incident beam was produced by an FEL lamp, located 3 m away from the detector. As shown in figure 2, at 0° tilt (see legend), the angular response curve is flattened around the 0° incidence angle because part of the reflected incident beam escaped through the entrance aperture of the sphere. The curve normalization was performed at the 0° incidence angle. As a result of this problem, the angular responsivity is different from the cosine function, the ideal angular responsivity of detector irradiance measurements. The difference from the cosine is about 0.2% at +4° and −4° incidence angles. The structures within the response curve are dominated by lamp instabilities.

In the following steps, the angular responses of the Ge sphere detector were measured at different aperture tilt angles (between the normal of the aperture plane and the sphere axis). The tilt angles were increased to check if the angular response relative to the above measurement (at 0° tilt) can be improved. The incidence angle (x-axis) was changed as above, by rotating the sphere detector around the centre of the sphere aperture. During these angular response scans, the sphere detector was rotated in a plane perpendicular to the plane where the entrance and the exit ports are. The normal of the aperture plane was increased from 0° (relative to the sphere axis) to 18° in increments shown in figure 2. During the angular response tests, at all tilt angles, the incident beam (at the 0° incidence angle) was always perpendicular to the plane of the input aperture. The measured response curves are shown in a ±10° range of the incidence angle. At a large enough tilt angle of the aperture plane (relative to the sphere axis), the angular response curve becomes similar to the cosine function. For aperture-plane tilt angles of 12° and 18°, the first specular reflection from the sphere wall could not escape from the sphere (as it happened at 0° tilt), therefore the normalized responses no longer show a suppressed cosine curve. The reason for the slight angular shift relative to the cosine function

[1] Certain commercial equipment, instruments or materials are identified in this paper to foster understanding. Such identification does not imply recommendation or endorsement by the National Institute of Standards and Technology, nor does it imply that the material or equipment are necessarily the best available for the purpose.

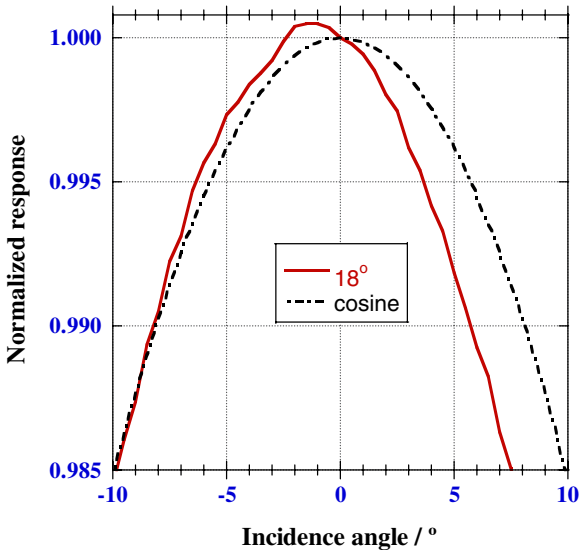

Figure 3. Angular response of a traditional Ge sphere detector where the 90° separated entrance and exit ports are in the plane of the rotation.

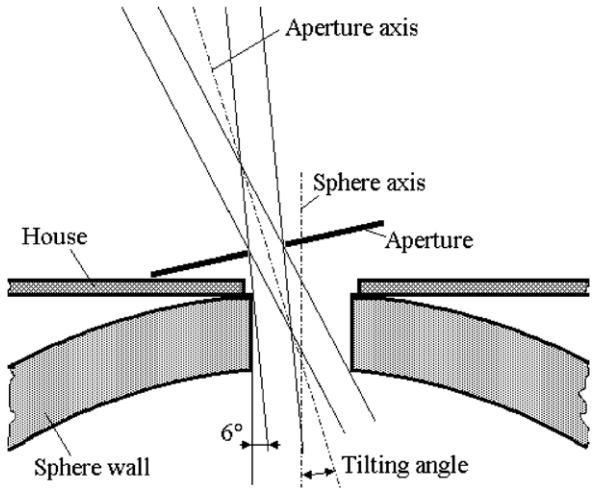

Figure 4. Sphere detector with a tilted aperture input.

is a close to 1° alignment error in the rotation of the sphere detector.

The above spatial and angular responsivity results show that traditional sphere detectors, with 90° angle between the entrance and exit ports and where the aperture plane is perpendicular (not tilted) to the sphere axis, have significant spatial and angular responsivity errors; therefore, they are not suitable for absolute power and irradiance mode measurements with the required less than 0.1% ($k = 2$) responsivity uncertainty. It has also been shown with the preliminary angular response tests (at different aperture tilt angles relative to the sphere axis) that the non-Lambertian angular response can be significantly improved if the input-aperture plane is tilted at least 12° relative to the sphere axis. This improvement was verified in the rotation plane perpendicular to the plane where the aperture and the detector are located.

The influence of the sphere-detector asymmetry (90° between the sphere aperture and the detector) for the angular response was tested as well. This test was performed with the 18° tilt (of the aperture plane relative to the sphere axis) in the plane where the aperture and the detector are located. To make this test, the previous angular response measurements were repeated after a 90° rotation of the sphere detector (around its optical axis) and the previous measurement geometry (pivot point and fixed lamp distance) was used again. The obtained angular response curve significantly deviated from the cosine function. The measured asymmetric curve is shown in figure 3 (at 18° tilt of the aperture plane relative to the sphere axis). The asymmetric angular response is caused by the asymmetric arrangement of the sphere entrance and exit ports in the plane of the rotation. (The rotation changes the incidence angle.) The deviation from the cosine is about 0.4% at a 4° incidence angle. This error in the angular responsivity can be significantly decreased if multiple detectors are symmetrically arranged relative to the incident-beam-produced spot on the sphere wall. A symmetrical detector arrangement can improve the spatial uniformity of responsivity as well.

The preliminary angular response measurement results verified that using 18° tilt in the plane of the input aperture (relative the sphere axis), the escaping radiation can be trapped and the angular responsivity to the cosine can be restored. Probably, there is a very small enhanced reflection peak at 0° in the BRDF of the Spectralon wall-coating since this material is not an ideal Lambertian reflector. This material characteristic produced the flattened angular response. Also, the trapped specular component of the first reflection could improve the spatial uniformity of responsivity which is important for low-uncertainty radiant power measurements. The results in figure 3 show that the traditional 90° aperture-detector arrangement should be changed to a symmetrical detector arrangement relative to the incident-beam-produced spot on the back of the sphere wall. A symmetrical detector arrangement can be implemented using multiple detectors instead of a single-element detector.

3. Design of the sphere-InGaAs radiometer

In order to improve the spatial and angular uniformity of the responsivity and to obtain lower responsivity uncertainties in a calibration transfer, a NIR transfer standard radiometer has been designed. The new radiometer has an integrating-sphere receiver with the optical axis of the entrance aperture tilted away from the sphere axis. Four temperature-controlled InGaAs photodiodes, selected for high shunt resistance, are symmetrically positioned in the sphere wall around the incident beam spot such that they cannot see each other.

The geometrical arrangement for the input of the sphere detector is shown in figure 4. A new position is needed for the aperture to obtain the maximum useful acceptance angle without beam clipping and to avoid any flux loss through the entrance aperture owing to the back reflection of the specular component of the incident beam from the sphere wall. The tilted aperture and the two unclipped beam-limits are illustrated. The incidence angle of the left limit-beam (relative to the sphere axis) is 6°, the other side limit-beam is determined by the sphere wall. The new entrance axis of

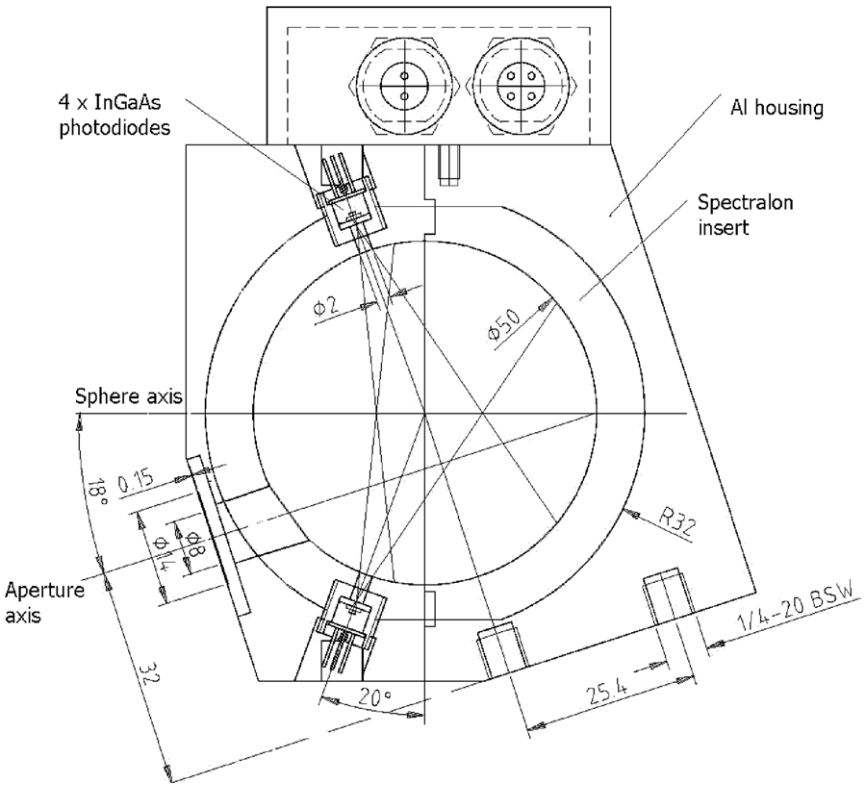

Figure 5. Cross-section of the sphere-InGaAs detector.

the sphere is the aperture axis, which splits the angle between two limit-beams. The measurements and calculations for the available components showed that the optimum value of the angle between the sphere axis and the aperture axis is 17.5°.

The cross-section of the sphere-InGaAs detector housing is shown in figure 5. The aperture axis is tilted by 18°. The housing is temperature controlled with a thermoelectric (TE) cooler/heater attached to the back of the Al-housing. As shown in the picture of the sphere detector in figure 6, a heat sink is attached to the back side of the TE cooler/heater. The four 1 mm diameter InGaAs detectors are selected for equal shunt resistance and they are parallel connected with each other. They are symmetrically positioned around the incident-beam-produced 'hot' spot such that they cannot see each other. The stabilized 26 °C temperature of the sphere housing propagates to the metal cans of the detectors.

4. Sphere-InGaAs radiometer characterizations

In figure 6, the sphere-InGaAs detector with a 5 mm diameter input aperture was characterized at the Spectral Comparator Facility (SCF) by scanning with a 1 mm diameter beam. The measured spatial uniformity at 1200 nm is shown in figure 7. The maximum-to-minimum responsivity change is less than 0.05%. The spatial uniformity tests were repeated at 1000 nm and 1600 nm. The pattern of the spatial non-uniformity of responsivity was different at each wavelength. The maximum-to-minimum responsivity change was also 0.05% at 1000 nm and it increased to 0.075% at 1600 nm. With a larger beam spot positioned in the aperture-centre, the beam positioning

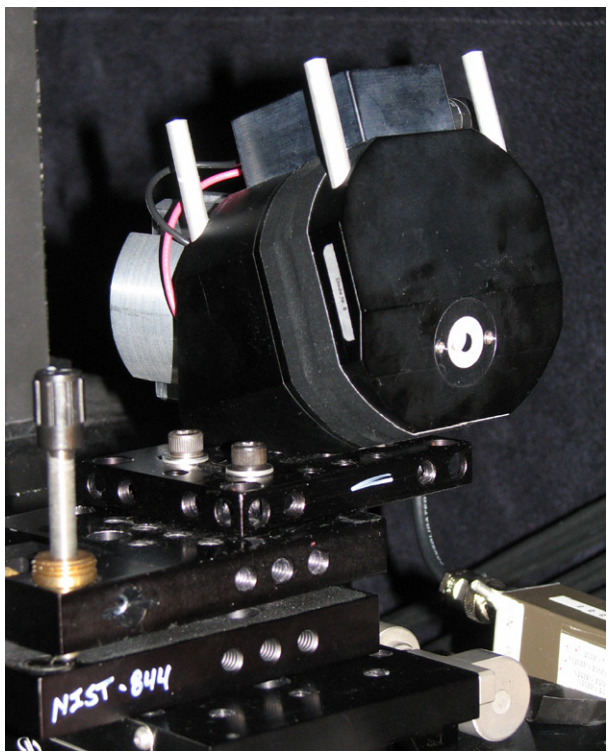

Figure 6. Picture of the sphere-InGaAs detector.

error in the power responsivity measurement can be decreased by about a factor of two.

The noise-equivalent-power (NEP) was determined from output noise and spectral power responsivity measurements

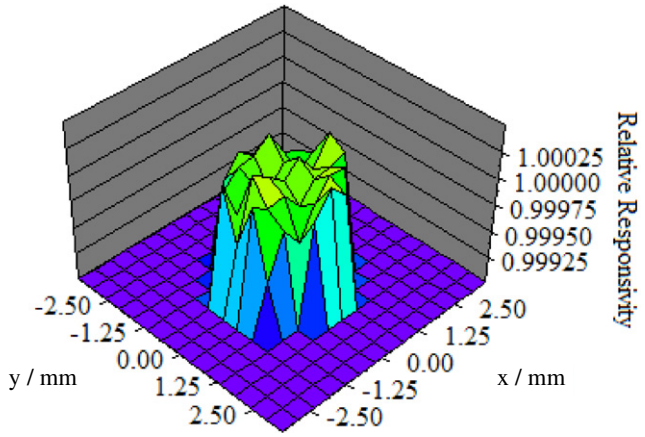

Figure 7. Spatial uniformity of the sphere-IGA detector with a 5 mm diameter input aperture at 1200 nm.

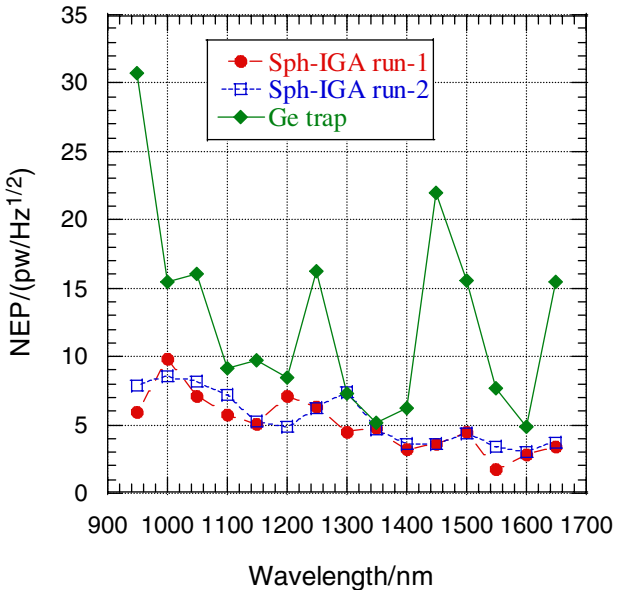

Figure 8. NEP comparison of the sphere-IGA and the Ge-trap detectors.

between 950 nm and 1650 nm. Figure 8 shows the NEP results from two spectral scans compared with the NEP of a Ge trap detector [8]. The obtained data verify that the dominating noise of the sphere-InGaAs detector is white noise, specifically resistor noise. The resistor noise, which originates from the parallel connection of the shunt resistance and the feedback resistance, is dominated by the resultant shunt resistance of the four parallel connected 1 mm detectors. The resultant shunt resistance was 33 MΩ for four non-selected photodiodes (set 1) and 50 MΩ for four photodiodes selected for equal shunt resistance of 200 MΩ (set 2). The expanded uncertainty of the shunt resistance measurements was 10% ($k = 2$). The feedback resistance of the current-to-voltage converter during the spectral measurements was 100 MΩ. The average NEP was 5 pW $Hz^{-1/2}$ for run 1 and 5.5 pW $Hz^{-1/2}$ for run 2 using set 1 with the 33 MΩ shunt resistance. Since the resultant shunt resistance of the Ge trap detector is only 1 kΩ, its dominating noise is $1/f$ noise. The $1/f$ noise determined NEP of the Ge trap detector was 30 pW $Hz^{-1/2}$.

Figure 9 shows the repeatability of four spectral responsivity scans at the SCF. The responsivity differences shown on the Y-axis are in the 0.05% level between 950 nm and 1350 nm and also between 1450 nm and 1650 nm. The larger differences at 1400 nm are caused by the atmospheric absorption.

The sphere-InGaAs detector angular responsivities were measured on a photometer bench. The illuminating source was a Wi41G lamp. This lamp had significantly smaller intensity fluctuations than the FEL lamp used in the preliminary experiments shown in figure 2. Otherwise, these measurements were performed similarly to the preliminary tests. Since the separation between the lamp and the sphere detector was about 3 m, the lamp operated like a 'point source' for the sphere-InGaAs detector. Two baffles were located between the lamp and the sphere detector to minimize stray light on the detector. The detector was mounted on a rotation stage and it was rotated around the aperture-centre in the horizontal plane. To repeat the angular responsivity measurements in the vertical plane, the sphere detector was 90° rotated on the rotation stage around its optical axis. The measurement results are shown in figure 10. The ratios of the measured responses to the cosine function are shown versus the rotation (incidence) angle of the sphere-InGaAs detector. The curves are normalized. The deviations from the cosine function are 0.03% if the (full-angle) field-of-view of the sphere-InGaAs detector is limited to 5°.

The long-term stability of the sphere-InGaAs detector is an important issue. Our two-years long stability tests on several InGaAs makes and models verified that these photodiodes (even if they are not temperature stabilized) exhibit less than 0.2% instabilities between 1.0 µm and 1.6 µm. Also, when measurements are not performed, a protecting cap is mounted to the entrance port of the sphere to keep the dust and dirt outside. The low NEP (high sensitivity) makes it possible to decrease throughput changes with grey sphere coatings where the reflectance factors are significantly smaller than unity. The sphere-InGaAs detector will be calibrated against the cryogenic radiometer yearly to calibrate out long-term changes.

5. Calibration procedure

The SIRCUS scale derivation is illustrated in figure 11. The new sphere-InGaAs detector (shown with the earlier used 90° aperture-detector arrangement) is calibrated against the cryogenic radiometer for absolute spectral power responsivity. Following the radiant power responsivity scale transfer, an irradiance mode tie point is derived from a silicon trap detector at about 950 nm. An alternative solution is to use an area-calibrated aperture in front of the sphere detector for power-to-irradiance mode conversion. The irradiance mode sphere-InGaAs detector is the reference detector for the SIRCUS in the NIR range to 1650 nm.

Other (test) irradiance detectors can be calibrated against the sphere-InGaAs reference detector when they both measure the irradiance from an integrating-sphere source of the SIRCUS. For absolute radiance responsivity calibrations,

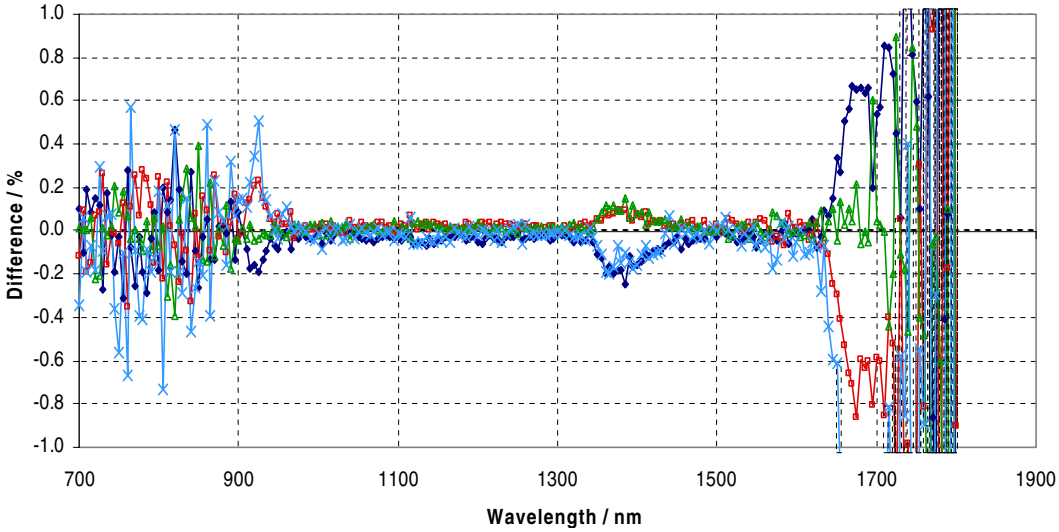

Figure 9. Responsivity differences (repeatability) of four spectral responsivity scans.

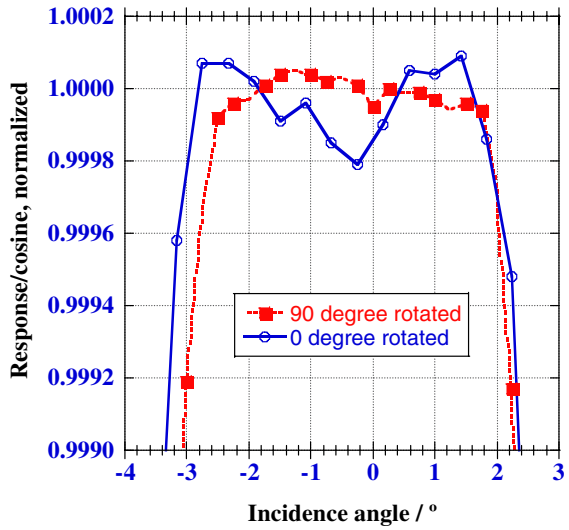

Figure 10. Response/cosine versus incident angle to the normal of the 8 mm diameter input aperture of the sphere detector.

a large sphere source is used at SIRCUS and its exit-port radiance is determined against the new sphere-InGaAs detector when the distance d is measured between the source aperture and the detector aperture. Test radiance meters are calibrated against the detector-based radiance of the large sphere source. In order to achieve the required 0.05% ($k = 2$) absolute radiance responsivity uncertainty, the uncertainty components are kept small and the sphere-InGaAs detector will not limit the overall uncertainty of the responsivity scale transfer.

6. Future applications

In addition to the SIRCUS irradiance and radiance responsivity scale extension to the NIR, the sphere-InGaAs detector can be used for fibre coupled spectral power responsivity scale transfer with sub-picowatt NEP and high coupling efficiency. The sphere-InGaAs detector with the 0.05% ($k = 2$) radiance responsivity uncertainty can also be used to determine the thermodynamic temperature of a 157 °C indium point (blackbody radiator) with 10 mK ($k = 2$) uncertainty. Also, because of its excellent spatial uniformity of responsivity, it can be applied for international spectral power responsivity comparisons with decreased uncertainties compared with presently used single-element or trap NIR quantum detectors even if the incident beam sizes are different (as was the case in the CCPR K2.a). We are planning to increase the area of the InGaAs detectors to increase responsivity. Also, the detectors will be cooled to increase their shunt resistance and to obtain lower output noise. According to our estimation, the NEP of an improved sphere-InGaAs detector can be as low as 50 fW $Hz^{-1/2}$. This is equal to the NEP of silicon tunnel-trap detectors built with shunt-resistance selected photodiodes. We also plan to extend the spectral range to 2.5 µm using cooled extended-InGaAs detectors.

7. Conclusions

This is the first time that a NIR transfer standard detector with similar performance to silicon trap detectors has been developed. Recent responsivity scale realizations on the SIRCUS facility demonstrated that silicon trap detectors can propagate the low-uncertainty radiant power scale of the cryogenic radiometer to 960 nm with a minimal increase in the uncertainty. Because of the increasing demand for less than 0.1% ($k = 2$) responsivity calibrations at the SIRCUS facility between 950 nm and 1650 nm, a transfer standard NIR radiometer was needed that can propagate the primary responsivity scale similarly to the silicon trap detectors. A novel sphere-input radiometer (with tilted input aperture to the sphere axis and a symmetrical arrangement of four InGaAs detectors to the incident beam spot on the sphere wall) has been developed with electronic and radiometric characteristics similar to silicon trap detectors. The two dominant responsivity uncertainty components (originating from the spatial non-uniformity and the angular responsivity

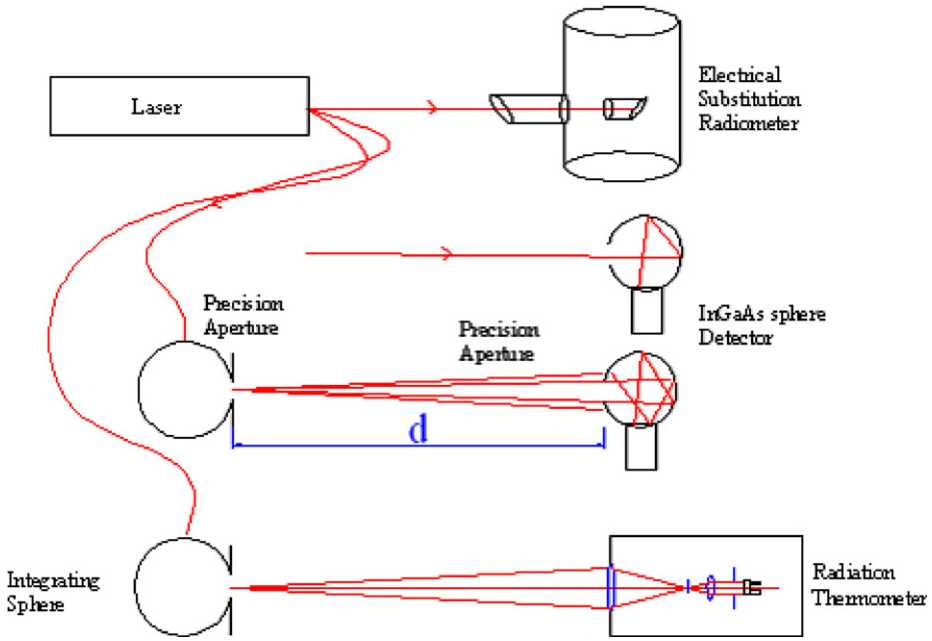

Figure 11. The SIRCUS responsivity scale derivation using a sphere-InGaAs detector.

deviation from the cosine) in a power to irradiance/radiance scale transfer could be decreased to less than 0.05% ($k = 2$). The new device with its improved responsivity uncertainty is used as the highest level reference radiometer of the SIRCUS facility for NIR irradiance and radiance mode spectral responsivity calibrations. The radiometer standard can be utilized to realize a detector-based radiation temperature scale down to 157 °C with a 10 mK ($k = 2$) uncertainty. There are also other application areas, such as fibre coupled spectral power responsivity measurements where the coupling efficiency can be high using this sphere-input standard. It also can be used as a travelling transfer detector to compare international NIR responsivity scales in both power and irradiance measurement modes with significantly lowered responsivity uncertainties.

References

[1] Zalewski E F and Duda C R 1983 Silicon photodiode device with 100% external quantum efficiency *Appl. Opt.* **22** 2867–73

[2] Brown S W, Eppeldauer G P and Lykke K R 2006 Facility for spectral irradiance and radiance responsivity calibrations using uniform sources *Appl. Opt.* **45** 8218–37

[3] Stock K D, Heine R and Hofer H 2003 Spectral characterization of Ge trap detectors and photodiodes used as transfer standards *Metrologia* **40** S163–6

[4] Lopez M, Hofer H and Kuck S 2006 High accuracy measurement of the absolute spectral responsivity of Ge and InGaAs trap detectors by direct calibration against an electrically calibrated cryogenic radiometer in the near-infrared *Metrologia* **43** 508–14

[5] Lamminpaa A, Noorma M, Hyyppa T, Manoocheri F, Karha P and Ikonen E 2006 Characterization of germanium photodiodes and trap detector *Meas. Sci. Technol.* **17** 908–12

[6] Carrasco-Sanz A, Rodríguez-Barrios F, Corredera P, Martín-López S, González-Herráez M and Luisa Hernanz M 2006 An integrating sphere radiometer as a solution for high power calibrations in fiber optics *Metrologia* **43** S145–50

[7] Boivin L P 2000 Properties of sphere radiometers suitable for high-accuracy cryogenic-radiometer-based calibrations in the near-infrared *Metrologia* **37** 273–8

[8] Lehman J H and Li X 1999 A transfer standard for optical fiber power metrology *Appl. Opt.* **38** 7164–6